Available online at www.sciencedirect.com
ScienceDirect
Proceedings of the Combustion Institute 000 (2022) 1–10
Proceedings of the Combustion Institute
www.elsevier.com/locate/proci

Dynamics and structure of detonations in stratified product-gas diluted mixtures

Davy Brouzet [a,b,*], Guillaume Vignat [a], Matthias Ihme [a]

[a] Department of Mechanical Engineering, Stanford University, Stanford, CA 94025, USA
[b] Center for Turbulence Research, Stanford University, Stanford, CA 94025, USA

Received 5 January 2022; accepted 19 July 2022
Available online xxx

Abstract

The dynamics and structure of detonations in stratified, product-gas diluted mixtures are examined using high resolution two-dimensional simulations with detailed chemistry. A stoichiometric methane/oxygen/nitrogen mixture with a product-gas dilution level similar to that found in rotating detonation engines is considered. A parametric analysis of the stratification size is performed. For stratification sizes larger than the induction length l_{ind}, the traditional detonation cell structure is lost and triple-points are absent. For stratification sizes an order of magnitude larger than l_{ind}, large regions of unburned, cold gases are found far behind the detonation front, and are subsequently consumed through an isobaric combustion process initiated by scalar mixing. This mechanism results in a deficit of energy provided to the detonation and to a significant reduction in the overall detonation velocity. A one-dimensional model using ZND theory is constructed to gain insights on the transient detonation structure. This model predicts a slower detonation velocity through the cold gases, which is supported by the results from the simulations with large stratification sizes. In these cases, the detonation structure is well predicted by the model in the regions that undergo ignition by shock compression, i.e., for intermediate and high levels of product-gas dilution. In the absence of triple-points, the detonation structure and dynamics can be locally considered as quasi-one-dimensional. The model and simulation results have a larger discrepancy for small stratification sizes, implying that phenomena other than adiabatic shock compression, involving heat and/or mass transfer, might play a role to ignite the reactants.

Keywords: Detonation; Detonation velocity; Vitiated flows; ZND theory

1. Introduction

Over recent years, significant progress has been made towards overcoming scientific and engineering challenges of pressure-gain combustion for power generation and propulsion [1,2]. These efforts are motivated by their higher theoretical efficiency compared to isobaric combustion systems. A practical example is the rotating detonation engine (RDE), which is a conceptually simple implementation of pressure-gain combustion, requiring no moving parts and providing a near-continuous thrust output. An RDE typically

* Corresponding author at: Department of Mechanical Engineering, Stanford University, Stanford, CA 94025, USA.
E-mail address: dbrouzet@stanford.edu (D. Brouzet).

https://doi.org/10.1016/j.proci.2022.07.173
1540-7489

consists of an annular combustion chamber that is continuously fueled by the injection of premixed or non-premixed reactants at the head plane. Depending on the operating conditions, one or multiple detonation waves propagate along the azimuthal direction close to the injection plane. It has been observed, both experimentally [3,4] and through simulations [5–7] that the wave velocity is significantly lower than the theoretical value estimated using Chapman–Jouguet (CJ) theory. Bennewitz et al. [3] report experimentally measured wave velocities as low as $0.33D_{CJ,0}$ in RDEs, where $D_{CJ,0}$ is the theoretical CJ detonation velocity through an unburned and perfectly premixed mixture.

This discrepancy in detonation velocity has been attributed, at least partially, to incomplete mixing of the reactants and to the dilution with combustion products (i.e., preburning) [8]. Because of the short residence time between injection and combustion, injection systems typically used in RDEs are prone to incomplete mixing [7,9]. The injector flow rates tend to be highly perturbed by the strong pressure variations associated with the passage of the detonation waves [10]. These effects lead to highly inhomogeneous mixtures that are composed of unburned fuel, oxidizer, and combustion products. The detonation waves therefore propagate in a complex stratified, vitiated, and preburned medium. Understanding and accurately predicting the effect of such mixtures on combustion efficiency remains an open research issue.

A series of one-dimensional (1D) and two-dimensional (2D) simulations were performed to analyze the impact of discrete energy sources embedded in an inert medium on the detonation structure and dynamics [11–13], showing that transverse waves and triple-points were weaker or even absent. In addition, inhomogeneities significantly larger than the induction length, led to an increase in the average detonation velocity. This result is consistent with theory when considering the propagation of a detonation in a weakly equivalence-ratio-stratified medium [14]. In a similar configuration with varying upstream fuel mass fraction, it was observed that faster auto-ignition accelerated the detonation front in high reactivity regions [15]. Even though the aforementioned studies examined inhomogeneous reactant mixtures, they did not consider preburning effects.

Experimentally investigating the detonations with well-controlled stratified, preburned mixtures is challenging and only a few numerical investigations have been attempted to study the effects of such media on detonations. Fujii et al. [5] made an effort in this direction by performing 2D simulations of a canonical RDE configuration and found that the detonation velocity was reduced to a minimum of $0.84D_{CJ,0}$ if reactants were injected in a non-premixed manner. However, the same system with premixed injection led to a detonation propagating at the CJ velocity, suggesting that the velocity deficit may have been caused by poor mixing and not by the presence of burned gases between the injectors. Prakash et al. [7] also studied the detonation propagation through stratified mixtures, which contained both equivalence ratio and combustion product gradients. While the equivalence ratio field was isotropic, the preburning profile was only varying in the detonation-normal direction. These results showed that the most probable detonation speed was close to the average preburned CJ value, even though significant fluctuations were observed.

While these studies have shown that combustion gas mixtures can result in slower detonation waves compared to fresh gas mixtures, the effects of equivalence ratio and preburning stratification have not been studied independently. In addition, a study of the detonation dynamics propagating through a streamwise and transverse stratified preburned medium, which is more representative of RDEs, is still lacking. It is also unclear if the long-standing Zeldovich–Neumann–Döring (ZND) theory is representative for such detonations. To address these questions and to assess the effects of inhomogeneities on the detonation speed and structure, we conduct 2D simulations of detonations through preburned mixtures using detailed chemistry. The numerical method and configuration are presented in Section 2. Results are discussed in Section 3, providing comparison to experimental data and detailed analysis of the detonation dynamics. Finally, conclusions of this study are presented in Section 4.

2. Numerical methods

A fully compressible finite-volume solver is used to conduct the simulations [16]. It solves the Navier–Stokes equations for conservation of mass, momentum, energy, and species:

$$\partial_t \rho + \nabla \cdot (\rho \boldsymbol{u}) = 0, \tag{1}$$

$$\partial_t (\rho \boldsymbol{u}) + \nabla \cdot (\rho \boldsymbol{u}\boldsymbol{u}) = \nabla \cdot (\boldsymbol{\tau} - p\boldsymbol{I}), \tag{2}$$

$$\partial_t (\rho e_t) + \nabla \cdot [\boldsymbol{u}(\rho e_t + p)] = \nabla \cdot [(\boldsymbol{\tau} \cdot \boldsymbol{u}) - \boldsymbol{q}], \tag{3}$$

$$\partial_t (\rho Y_k) + \nabla \cdot (\rho \boldsymbol{u} Y_k) = -\nabla \cdot \boldsymbol{j}_k + \dot{\omega}_k, \tag{4}$$

with density ρ, gas velocity vector $\boldsymbol{u}$, pressure p, and specific total energy e_t. The species equations are solved for $k = 1$ to $N_s - 1$, where N_s is the number of species and N_2 is the last species. The mass fractions and source terms for species k are denoted by Y_k and $\dot{\omega}_k$, respectively. The system is closed with the ideal gas equation of state. The stress tensor $\boldsymbol{\tau}$, the heat flux $\boldsymbol{q}$, and the diffusion flux for the kth species $\boldsymbol{j}_k$ are modeled as,

$$\boldsymbol{\tau} = \mu\left[\nabla \boldsymbol{u} + (\nabla \boldsymbol{u})^T\right] - \frac{2}{3}\mu(\nabla \cdot \boldsymbol{u})\boldsymbol{I}, \tag{5}$$

Please cite this article as: D. Brouzet, G. Vignat and M. Ihme, Dynamics and structure of detonations in stratified product-gas diluted mixtures, Proceedings of the Combustion Institute, https://doi.org/10.1016/j.proci.2022.07.173

$$\boldsymbol{q} = -\lambda_T \nabla T - \rho \sum_{k=1}^{N_s} h_k D_k \nabla Y_k, \tag{6}$$

$$\boldsymbol{j}_k = -\rho D_k \nabla Y_k, \tag{7}$$

where h_k is the partial enthalpy of species k. The dynamic viscosity μ and the thermal conductivity λ_T are evaluated using polynomial fits from CANTERA [17] subroutines. Diffusion coefficients D_k are computed using a mixture-averaged approximation. No turbulence or scalar subgrid scale models are used.

The equations are discretized using a hybrid scheme that combines a 4th order accurate central spatial scheme with a 2nd order ENO reconstruction scheme in regions of high density and pressure gradients [16]. A Strang-splitting scheme is employed for time-advancement, combining a strong stability preserving 3rd order Runge–Kutta scheme for the non-stiff operators with a semi-implicit Rosenbrock–Krylov scheme for the chemical source terms [18]. This allows for a convective timestep of 3 ns, corresponding to a maximum CFL number of 0.45.

Two-dimensional simulations of detonations in homogeneous and inhomogeneous preburned mixture composition are performed. A $CH_4/O_2/N_2$ mixture is considered, with an equivalence ratio $\phi = 1$ and a 25% N_2 molar dilution. The unburned gases are at $T_u = 300$ K and $p_u = 22.2$ kPa to match the experimental data of Frederick et al. [19]. The composition of the preburned mixture is specified by considering the equilibrium composition from an isobaric combustion at the same initial state. The temperature T and species mass fractions are specified as:

$$\Theta(\xi) = \Theta_u + \xi(\Theta_{eq} - \Theta_u), \tag{8}$$

where the subscripts u and eq denote the unburned and equilibrium states, respectively, and $\Theta = \{T, Y_k\}$. The preburning factor $\xi \in [0, 1]$ represents the local fraction of combustion products. At the conditions considered, the equilibrium state is $T_{eq} = 2752$ K, $Y_{O_2,eq} = 0.0818$, $Y_{H_2O,eq} = 0.241$, $Y_{H_2,eq} = 4.24 \times 10^{-3}$, $Y_{CO,eq} = 0.126$, and $Y_{CO_2,eq} = 0.184$, with N_2 as the remaining balance. While radicals in the vitiated mixture can potentially reduce induction times, they are not considered in this configuration as they lead to autoignition in the region ahead of the detonation. This early combustion was likely the result of high radical concentrations. Additional experimental data or parametric studies are required to estimate radical concentrations comparable to the ones found in practical configurations.

Two homogeneous conditions with $\xi = 0$ and $\xi = 0.5$ are considered, the latter being representative of preburning levels encountered in RDEs [7]. To analyze the effects of preburned inhomogeneities on the detonation behavior and detonation structure, additional cases with an average preburning factor of $\xi_0 = 0.5$ are considered, in which the preburned field is prescribed by the following function:

$$\xi(x, y) = \xi_0 \left[1 + \sin\left(\frac{2\pi y}{\lambda}\right) \sin\left(\frac{2\pi x}{\lambda}\right) \right], \tag{9}$$

where λ is the characteristic wavelength. Mi et al. [11], 12] observed that the detonation response to energy inhomogeneities was dependent on the ratio λ/l_{ind}, where l_{ind} represents the induction length of the partially burned mixture. We therefore perform a parametric study on the size of the inhomogeneities, with $\lambda/\, l_{ind} = \{0.7, 1.7, 4.2, 11\}$, the latter being of the order of the detonation cell [20]. In the following, we refer to the homogeneous case as $\lambda/l_{ind} = \infty$, since $\xi(x, y) \to \xi_0$ in the limit of $\lambda \to \infty$.

Considering CH_4/air detonations, Wang et al. [21] found that the transient detonation dynamics were considerably different for simplified and detailed (i.e., $\geq$ 20 species) mechanisms, arising from substantial differences in the ignition delay predictions. In order to accurately simulate the detonation dynamics, a 20-species, 97-reactions skeletal mechanism [22], derived from the GRI3.0 mechanism, is therefore used. Comparisons between the skeletal mechanism and the experimental data of Hu et al. [23] showed good agreement in ignition delays. Further comparison to the experimental data of Frederick et al. [19] is performed in Section 3.1 to assess the accuracy of the mechanism and the numerical methods.

A 2D rectangular $x - y$ domain of streamwise and transverse lengths $L_x = 70$ mm and $L_y = 100$ mm, respectively, is considered. These dimensions were found to be adequate so that the reactants are entirely consumed before reaching the outlet and that at least three detonation cells are present along the y-direction. The latter requirement ensures that the boundaries in the transverse direction do not influence the detonation cellular structure [24].

The right-inflow conditions are specified by a Navier–Stokes Characteristic Boundary Condition (NSCBC) formalism for compressible, multi-species flows [25]. Symmetry conditions are imposed at the transverse boundaries. The left-outflow boundary requires special attention, as changes of the back pressure can result in acoustic or rarefaction waves that affect the detonation front. Therefore, NSCBC non-reflecting boundary conditions are used, where the pressure is relaxed to the theoretical CJ pressure if the flow is locally subsonic. The relaxation factor chosen corresponds to a timescale of 50 μs, which is significantly larger than the timescales associated with the detonation cells, to ensure that the relaxation does not affect the detonation dynamics. A schematic of the domain with relevant boundary conditions information is displayed in Fig. 1

Please cite this article as: D. Brouzet, G. Vignat and M. Ihme, Dynamics and structure of detonations in stratified product-gas diluted mixtures, Proceedings of the Combustion Institute, https://doi.org/10.1016/j.proci.2022.07.173

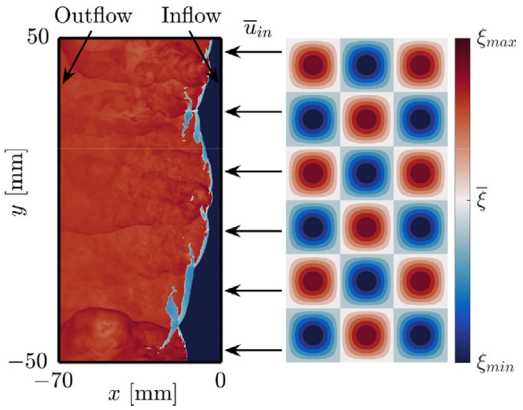

Fig. 1. Schematic of the configuration.

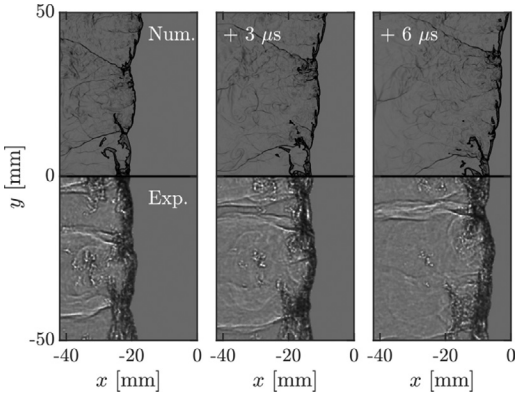

Fig. 2. Comparisons of instantaneous Schlieren results for the homogeneous case with $\xi = 0$ between simulations and experiments [19]. The snapshots are separated by 3 μs and the numerical Schlieren results are computed as $\exp(-|\nabla\rho|/|\nabla\rho|_{\max})$.

To stabilize the detonation front, we adopt the method by Gamezo et al. [24], where the inflow velocity is imposed at a constant value of $\overline{u}_{in} = -2100$ m/s $\approx D_{CJ,0}$. If the leading detonation front is located too close or too far from the inflow, the computational domain is translated in the x-direction to shift the detonation. Extensive testing was performed to ensure that this methodology did not induce spurious fluctuations that could affect the detonation.

The domain is discretized using a Cartesian mesh with $N_x = 800$ and $N_y = 2000$ cells, and a uniform spacing of 50 μm in the first 25 mm, where the detonation front is located. The spacing along the streamwise direction is then gradually increased to a maximum of 150 μm. The resolution in the detonation region corresponds to at least 60 cells per l_{ind}, as recommended by Sharpe [26] to resolve the triple-point dynamics. At least 3 cells per exothermic length are guaranteed with the current resolution. Data is collected for at least 70 μs once the statistically stationary state is reached, which is assessed based on the detonation velocity and average outflow pressure.

3. Results

3.1. Comparison with experimental data

In this section, detonation dynamics of the case with a homogeneous mixture at $\xi = 0$ are compared to experimental results [19] to assess the numerical methodology described in Section 2. The experiments were conducted at the GALCIT Narrow Channel Facility, which is a high aspect ratio, rectangular channel. This configuration effectively suppresses spanwise wave motions across the width of the channel, generating a 2D detonation structure across the channel height. Details about the experimental apparatus and methodology can be found in [19].

Comparisons of numerical Schlieren results with measurements are presented in Fig. 2, showing three flow fields that are separated by 3 μs. The development of a detonation cell as two triple-points propagate in opposite directions is observed. The overall detonation structure including the presence of triple-points, transverse waves phenomena and Mach stem is observed in the simulation and qualitatively similar to the measurements.

For further comparisons, the numerical results are post-processed to identify the local detonation front at every timestep using a pressure threshold-based algorithm. The streamwise detonation velocity D is then computed using a first-order Euler discretization. A more accurate algorithm was developed to identify the shock-normal speed but led to negligible differences. Maps for the spatially-reconstructed detonation velocities are then computed from the known upstream gas velocity, and comparisons with experimental data are shown in Fig. 3(a,b). The detonation velocity deficit reported is computed relative to $D_{CJ} = 2143$ m/s as $\Delta D = (D - D_{CJ})/D_{CJ}$.

Both maps show cell regions of varying sizes with lower local velocities. Diagonal lines, corresponding to propagating triple-points, have a positive deficit. The maps are qualitatively similar even though the cell structure is better identified in the simulations. Considering the probability density functions (pdfs) of these maps in Fig. 3(c), a good agreement between numerical and experimental results is observed. In both cases, the mean detonation velocity deviates by less than 4% compared to D_{CJ} and variations in peak values range from −40% to +50%. Overall, these comparisons show that the detonation dynamics are well represented by the simulation.

Please cite this article as: D. Brouzet, G. Vignat and M. Ihme, Dynamics and structure of detonations in stratified product-gas diluted mixtures, Proceedings of the Combustion Institute, https://doi.org/10.1016/j.proci.2022.07.173

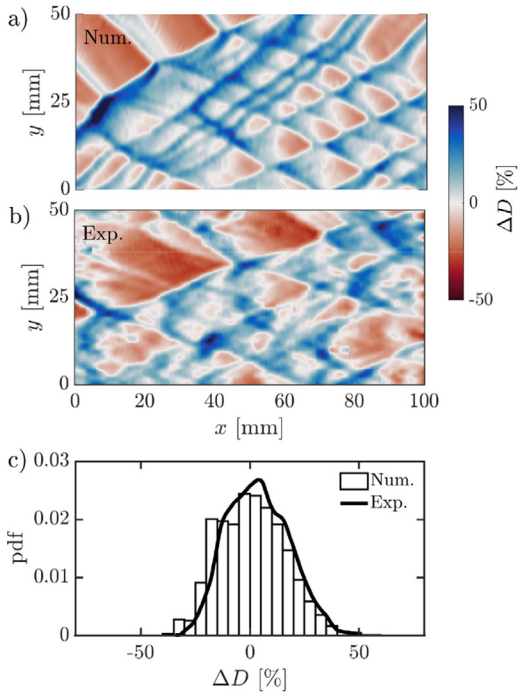

Fig. 3. a) Numerical and b) experimental spatial velocity deficit maps and c) corresponding pdf of velocity deficit.

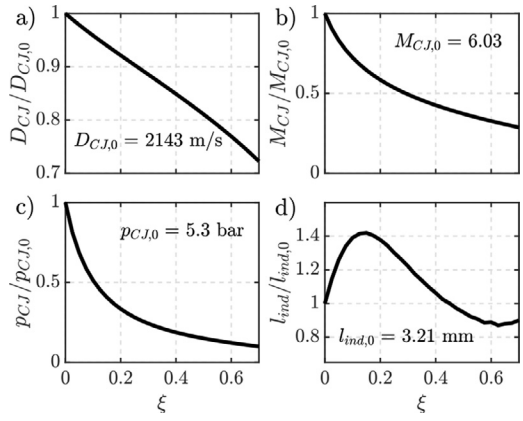

Fig. 4. Variation of a) the CJ detonation velocity, b) the CJ detonation Mach number, c) the CJ pressure, and d) the induction length, as a function of ξ. The quantities are normalized by the $\xi = 0$ values.

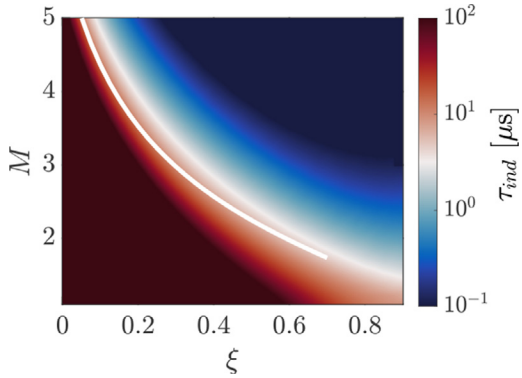

Fig. 5. Induction time obtained with the 1D detonation model, as a function of the detonation Mach number M and ξ. The white line shows the CJ solution.

3.2. One-dimensional detonation model

Before examining the simulation results, it is worth considering the effects of a homogeneous preburned field on 1D CJ detonation characteristics, which is assessed using the Shock and Detonation Toolbox [27]. The CJ detonation velocity D_{CJ}, CJ detonation Mach number $M_{CJ} = D_{CJ}/c_u$ (where c is the speed of sound), CJ pressure, and l_{ind} are shown in Fig. 4 as a function of ξ. While D_{CJ} decreases significantly, an even more drastic decrease is observed for M_{CJ}, as the sound speed in the upstream mixture increases with ξ because of the increasing temperature. A lower M_{CJ} implies a reduced pressure increase across the shock front, which explains the strong reduction in p_{CJ}. An increased ξ means a higher temperature of the reactants, which favors a smaller induction time. In contrast, increasing ξ leads also to more diluted reactants, which will decrease the reactivity of the mixture. These two effects compete against each other, and explain the non-monotonic and limited effect of ξ on the induction length. For the homogeneous case with $\xi = 0.5$ considered in this paper, the CJ conditions are $D_{CJ} = 1738$ m/s, $M_{CJ} = 2.24$, $T_{CJ} = 2863$ K, and $p_{CJ} = 0.86$ bar.

To gain a phenomenological understanding of the detonation structure in a stratified, preburned medium, the ZND theory is employed. Using this framework for CJ detonations, a quantity of interest ψ (e.g., the temperature profile or the induction time τ_{ind}) is function of M_{CJ} and the upstream conditions. In the context of homogeneous preburned mixtures at constant pressure, we therefore have $\psi = \psi(M_{CJ}(\xi), \xi) = \psi(\xi)$. To extend this methodology to stratified, preburned mixtures, we consider the detonation Mach number M as an independent variable, so that $\psi = \psi(M, \xi)$. The induction times obtained with this methodology are shown in Fig. 5. As previously observed in unstable detonations through homogeneous fields [28], a small reduction in the detonation Mach number induces a large increase in τ_{ind}.

Considering a multi-dimensional detonation propagating in a stratified field at constant pressure and constant heat capacity ratio γ, the von Neumann (i.e., frozen post-shock) state will be at equilibrium only if M is constant. Otherwise, the von Neumann pressure will vary, resulting in acoustic

Please cite this article as: D. Brouzet, G. Vignat and M. Ihme, Dynamics and structure of detonations in stratified product-gas diluted mixtures, Proceedings of the Combustion Institute, https://doi.org/10.1016/j.proci.2022.07.173

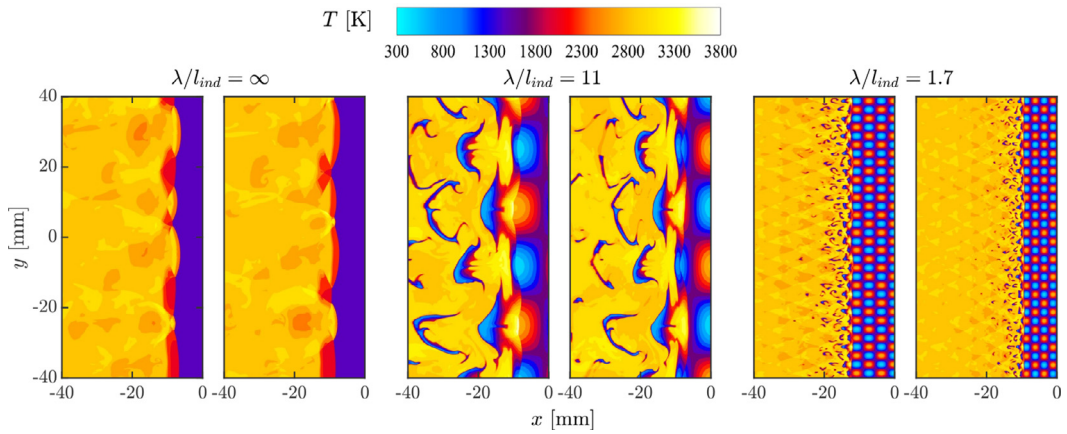

Fig. 6. Instantaneous temperature fields for $\lambda/l_{ind} = \{\infty, 11, 1.7\}$. The two snapshots shown for each case are 3 μs apart.

waves that will propagate across the ZND region and alter the detonation velocity. Considering this equilibrium state for a constant M, Fig. 5 shows that small changes in ξ introduce substantial variations in τ_{ind}. In addition, the lower temperature in the unburned gases results in extremely long τ_{ind}. These results suggest that the detonation behavior in a stratified, preburned field might be locally very different depending on the upstream mixture.

3.3. Detonation behavior in stratified ξ media

We examine the simulation results by considering instantaneous temperature fields for $\lambda/l_{ind} = \{\infty, 11, 1.7\}$, which are shown in Fig. 6. The two snapshots shown for each case are 3 μs apart. It is first noted that the case for $\lambda/l_{ind} = \infty$ is only weakly unstable, due to the low energy content of the $\xi_0 = 0.5$ mixture. Cellular structures are observed but unburned pockets behind the detonation front are absent. The introduction of large spatial inhomogeneities with $\lambda/l_{ind} = 11$ creates pockets of unburned, cold reactants far behind the shock front. These pockets are then slowly consumed downstream before exiting the domain. The same behavior, albeit at a much smaller scale, is observed in the case with $\lambda/l_{ind} = 1.7$. The fact that the fresh gases, which have the highest heat of combustion, do not detonate might seem counter-intuitive but can be explained by the 1D ZND model introduced in Section 3.2. Fig. 5has shown that for a given detonation Mach number, τ_{ind} was the greatest for low ξ. This result implies that the fresh mixture does not undergo ignition by adiabatic shock compression but is rather consumed through scalar mixing. This behavior is reminiscent of the mixing necessary to ignite unburned pockets in strongly unstable detonations in a homogeneous medium [28,29], even though the scales attained in the present configuration are significantly larger.

Table 1
Average detonation velocities. The percentages denote the relative difference compared to the case with $\lambda/l_{ind} = \infty$.

λ/l_{ind}	$\overline{D}$ [m/s]
0.7	1833 (+2.6%)
1.7	1835 (+2.7%)
4.2	1823 (+2.1%)
11	1714 (−4.0%)
∞	1786

Additional information about the global detonation structure can be obtained by considering numerical soot foils, which represent the maximum pressure achieved at every spatial point. Results for four cases considered are shown in Fig. 7. For $\lambda/l_{ind} = \infty$, the classical cellular detonation structure induced by the transverse propagation of triple-points is observed. At $\lambda/l_{ind} = 11$ and 1.7, triple-points are absent and a structure of the size of the stratification length emerges. A comparison to the temperature field shows that the regular, high-pressure patterns develop at conditions where the gases are at a low temperature. At $\lambda/l_{ind} = 0.7$, the cellular structure is observed again, implying that the triple-points are not affected by stratification sizes smaller than l_{ind}.

We proceed by examining the characteristics of the detonation velocity. Table 1 shows the average detonation velocity $\overline{D}$ for the different values of λ/l_{ind} considered. A slight increase in D is observed for inhomogeneities of size $\lambda/l_{ind} \leq 4.2$. This result echoes previous studies [11,30], which identified detonations in stratified mixture with average propagation speeds significantly greater than the CJ velocity. For sufficiently small inhomogeneities sizes, they established that the detonation behavior reverts to that of a homogeneous mixture. Their criterion was based on the ratio $\tau_c = t_r/t_s$, where t_r represents the heat release timescale and t_s is the

Please cite this article as: D. Brouzet, G. Vignat and M. Ihme, Dynamics and structure of detonations in stratified product-gas diluted mixtures, Proceedings of the Combustion Institute, https://doi.org/10.1016/j.proci.2022.07.173

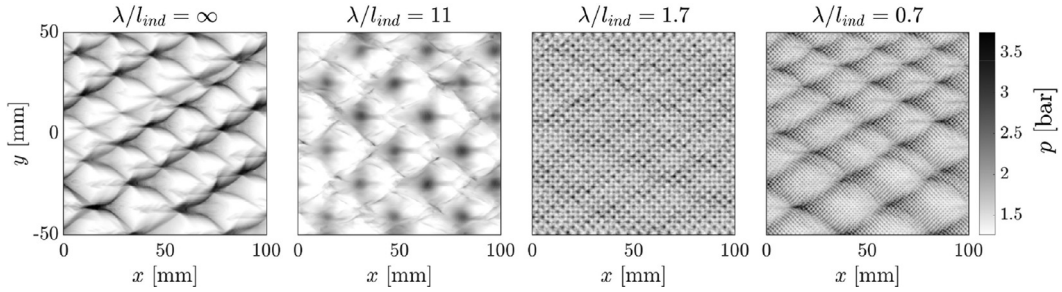

Fig. 7. Numerical soot foils for $\lambda/l_{ind} = \{\infty, 11, 1.7, 0.7\}$.

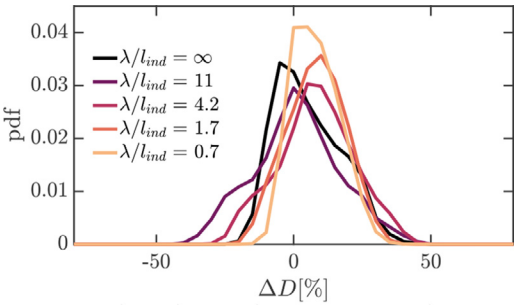

Fig. 8. Pdfs of the local detonation velocity deficit.

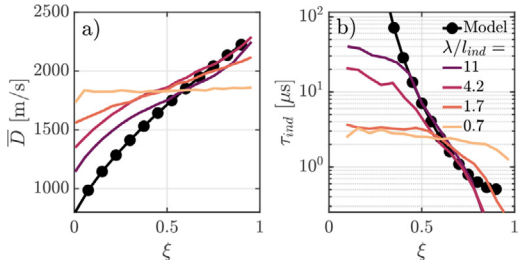

Fig. 9. a) Average local detonation velocity and b) induction time τ_{ind} conditioned on the upstream ξ.

convective time between inhomogeneities, i.e. $\lambda/\overline{D}$. The former can be estimated using the 1D model discussed in the present paper. For the smallest size $\lambda/l_{ind} = 0.7$, $t_r = 0.40\,\mu$s and $t_s = 1.21\,\mu$s, resulting in $\tau_c = 0.33$. According to Mi et al. [11], the convergence to the CJ speed occurs when τ_c is close to unity, explaining why the detonation with the lowest inhomogeneities size propagates still at a super CJ speed.

For $\lambda/l_{ind} = 11$, however, the inhomogeneities result in a significant decrease of the average detonation velocity. This deficit is likely due to the large amount of reactants that do not support the detonation propagation as they are consumed far from the shock front (see Fig. 6). Further insight can be gained by analyzing the pdfs of the detonation velocity deficit, shown in Fig. 8. While all distributions have a peak close to D_{CJ}, the amount of negative ΔD increases with λ. Therefore, the lower average velocity observed for $\lambda/l_{ind} = 11$ is mostly due to an increasing presence of very slow detonation fronts.

To understand why the detonation velocity deficit reaches such low values and to gain more insight about the effect of the upstream conditions, results of conditionally averaged D on ξ are shown in Fig. 9(a). The detonation velocity $D = Mc$ from the 1D ZND model is shown by the black line. A constant $M = 2.24$, which corresponds to the CJ Mach number in a homogeneous $\xi = 0.5$ mixture, was assumed. As the size of the inhomogeneities increases, D relaxes to the condition predicted by the model. This result implies that the detonation is locally at a post-shock equilibrium and therefore propagates at a constant Mach number for inhomogeneities with a characteristic size that is at least an order of magnitude larger than l_{ind}. According to the model and simulation results for $\lambda/l_{ind} \gg 1$, the detonation therefore propagates the slowest through the unburned gases and the fastest through regions with a high level of combustion products. When $\lambda/l_{ind} < 1$, however, the local detonation velocity becomes unaffected by the stratification and propagates at a nearly constant average velocity.

To quantify the effect of ξ on the local detonation structure, we adopt a Lagrangian framework where the position of a fluid parcel $\mathbf{x}(t)$ is computed by solving the differential equation $d\mathbf{x}/dt = \mathbf{u}(\mathbf{x}, t)$, for several initial positions ahead of the detonation front. Numerical integration is performed using a forward Euler scheme with a timestep of 0.2 μs and a 3rd order spatial interpolation. Extensive testings were performed to ensure that this numerical approach led to converged results. This methodology results in Lagrangian trajectories on which quantities of interest, such as the temperature and the pressure, can be obtained. In addition, the induction time along these trajectories can be computed and conditionally averaged based on the local ξ value at the initial position. These conditionally averaged τ_{ind} are shown in Fig. 9(b). Con-

Please cite this article as: D. Brouzet, G. Vignat and M. Ihme, Dynamics and structure of detonations in stratified product-gas diluted mixtures, Proceedings of the Combustion Institute, https://doi.org/10.1016/j.proci.2022.07.173

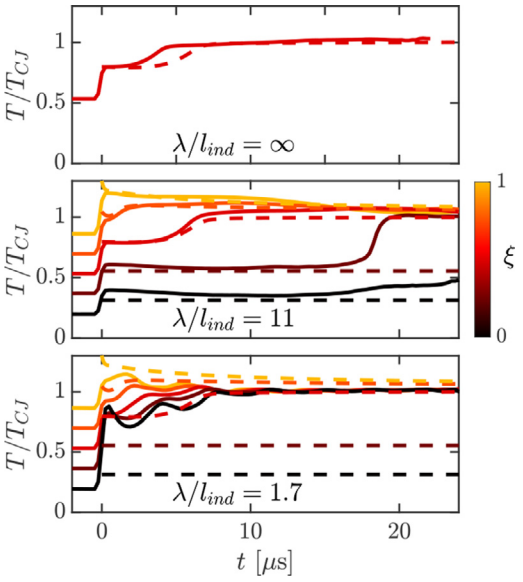

Fig. 10. Median numerical detonation structures for $\lambda/l_{ind} = \{\infty, 11, 1.7\}$. The dashed lines represent the 1D model with $M = 2.24$ and the line colors show the local upstream ξ value.

sidering the largest stratification size, one can notice the good agreement with the model for $\xi > 0.4$, implying that the detonation undergoes ignition via adiabatic shock compression in that range. As mentioned earlier, the model predicts very large induction times for low values of ξ and Fig. 6 showed that the reactants are consumed through scalar mixing. This different combustion process induces induction times that are much shorter than the ones predicted by the ZND model, of the order of 50 μs at maximum. The time necessary for the fresh gases to ignite decreases with λ, as the unburned gas pockets become smaller. To the limit where $\lambda/l_{ind} < 1$, the induction time becomes independent on the upstream value of ξ, again illustrating that the detonation is not affected by the mixture upstream of the detonation. In all cases however, it is clear that the fresh gases do not undergo ignition by adiabatic shock compression, illustrating the relevance of post-shock mixing to the dynamics of detonations in stratified media.

To illustrate how the von Neumann state and the detonation structure are affected by the inhomogeneities, median profiles of the temperature, conditioned on the upstream local value of ξ, are shown in Fig. 10. The dashed lines show the profiles from the 1D model and the time $t = 0$ denotes the moment the Lagrangian parcels pass through the shock front.

Results for $\lambda/l_{ind} = \infty$ show that the von Neumann and CJ states are well captured for this homogeneous case but the induction time is significantly lower than the theoretical value. Considering the case for $\lambda/l_{ind} = 11$ at intermediate values of ξ, the von Neumann state and subsequent rapid combustion can be clearly identified. This result contrasts with the profile for the lowest value of ξ, where the reactants have not been consumed after 25 μs, which is consistent with the results discussed in Fig. 9(b). In all cases that undergo ignition by adiabatic shock compression, i.e., for $\xi \geq 0.5$, the 1D model shows good agreement with the simulation results. As discussed in Fig. 7, triple-points are absent in the case with $\lambda/l_{ind} = 11$, meaning that the local detonation structure can be considered as a quasi-1D detonation. Even though the von Neumann state is in good agreement between the model and the simulations for the low preburned composition, the ignition stage is not well predicted by the model. This is expected since this region of the mixture does not undergo ignition by shock compression.

Finally, considering the profiles for the case with $\lambda/l_{ind} = 1.7$, it is observed that differences induced by the upstream mixture are reduced and all reactants are burned in less than 10 μs. The 1D model and simulations differ significantly, suggesting that for stratification sizes of the order of l_{ind}, phenomena other than shock compression, involving heat and/or mass transfer, may play a role in the von Neumann region.

4. Conclusions

Two-dimensional, high resolution simulations with detailed chemistry were performed to analyze the dynamics and structure of $CH_4/O_2/N_2$ detonations in stratified, product-gas diluted mixtures. First, the simulation results were compared to the experiments of Frederick et al. [19] for a homogeneous mixture composed of fresh reactants, showing good agreement on the local detonation velocity and cellular structure. Then, stratified mixtures with a product-gas dilution level similar to the ones found in RDEs were considered. A parametric analysis of the stratification size was performed.

For stratification sizes larger than but of the order of l_{ind}, the detonation cell structure was lost and triple-points were absent. For stratification sizes that were an order of magnitude larger than l_{ind}, the cold reactants did not undergo ignition via adiabatic shock compression and instead formed large unburned regions behind the detonation front. These pockets were subsequently burned through scalar mixing. This resulted in a deficit of energy provided to the detonation and a significant reduction in the average detonation velocity.

A 1D detonation model considering a von Neumann equilibrium state was constructed to gain insights on the detonation structure. This model predicted a slower detonation velocity through the cold gases, which was supported by the results from

Please cite this article as: D. Brouzet, G. Vignat and M. Ihme, Dynamics and structure of detonations in stratified product-gas diluted mixtures, Proceedings of the Combustion Institute, https://doi.org/10.1016/j.proci.2022.07.173

the simulations with large stratification sizes. In these cases, the detonation structure was well predicted by the model in the regions that ignited thanks to shock compression, i.e., for intermediate and high levels of product-gas dilution. The absence of triple-points meant that the detonation could be locally approximated by the 1D model. The model and simulation results had a larger discrepancy for the cases with a stratification size of the order of l_{ind}, implying that phenomena other than adiabatic shock compression, involving heat and/or mass transfer, might play a role to ignite the reactants in the von Neumann region.

Declaration of Competing Interest

The authors declare that they have no known competing financial interests or personal relationships that could have appeared to influence the work reported in this paper.

Acknowledgments

Financial support from the Air Force Research Laboratory under grant no. RAPF1-0000001326 and from the Air Force Office for Scientific Research under grant no. FA9550-21-1-0077 with Dr. Chiping Li as Program Manager is gratefully acknowledged.

Supplementary material

Supplementary material associated with this article can be found, in the online version, at doi:10.1016/j.proci.2022.07.173.

References

[1] F.K. Lu, E.M. Braun, J. Powers, Rotating detonation wave propulsion: experimental challenges, modeling, and engine concepts, J. Propuls. Power 30 (5) (2014) 1125–1142, doi:10.2514/1.B34802.
[2] A.R. Baratta, J.B. Stout, Demonstrated low pressure loss inlet and low equivalence ratio operation of a rotating detonation engine (RDE) for power generation, AIAA Paper, 2020. 2020–1173
[3] J.W. Bennewitz, B.R. Bigler, W.A. Hargus, S.A. Danczyk, R.D. Smith, Characterization of detonation wave propagation in a rotating detonation rocket engine using direct high-speed imaging, AIAA Paper, 2018, doi:10.2514/6.2018-4688. 2018–4688
[4] B.A. Rankin, D.R. Richardson, A.W. Caswell, A.G. Naples, J.L. Hoke, F.R. Schauer, Chemiluminescence imaging of an optically accessible non-premixed rotating detonation engine, Combust. Flame 176 (2017) 12–22, doi:10.1016/j.combustflame.2016.09.020.
[5] J. Fujii, Y. Kumazawa, A. Matsuo, S. Nakagami, K. Matsuoka, J. Kasahara, Numerical investigation on detonation velocity in rotating detonation engine chamber, Proc. Combust. Inst. 36 (2017) 2665–2672, doi:10.1016/j.proci.2016.06.155.
[6] C.F. Lietz, Y. Desai, W. Hargus, V. Sankaran, Parametric investigation of rotating detonation rocket engines using large eddy simulations, AIAA Paper, 2019, doi:10.2514/6.2019-4129. 2019–4129
[7] S. Prakash, V. Raman, C.F. Lietz, W.A. Hargus, S.A. Schumaker, Numerical simulation of a methane-oxygen rotating detonation rocket engine, Proc. Combust. Inst. 38 (2021) 3777–3786, doi:10.1016/j.proci.2020.06.288.
[8] F. Chacon, M. Gamba, Study of parasitic combustion in an optically accessible continuous wave rotating detonation engine, AIAA Paper, 2019, doi:10.2514/6.2019-0473. 2019–0473
[9] R. Bluemner, M.D. Bohon, C.O. Paschereit, E.J. Gutmark, Experimental study of reactant mixing in model rotating detonation combustor geometries, Flow Turbul. Combust. 102 (2) (2019) 255–277, doi:10.1007/s10494-018-9966-7.
[10] J. Burr, K.H. Yu, Mixing in linear detonation channel with discrete injectors and side relief, AIAA Paper, 2019, doi:10.2514/6.2019-1014. 2019–1014
[11] X. Mi, A.J. Higgins, H.D. Ng, C.B. Kiyanda, N. Nikiforakis, Propagation of gaseous detonation waves in a spatially inhomogeneous reactive medium, Phys. Rev. Fluids 2 (5) (2017) 053201.
[12] X. Mi, E.V. Timofeev, A.J. Higgins, Effect of spatial discretization of energy on detonation wave propagation, J. Fluid Mech. 817 (2017) 306–338.
[13] X. Mi, A. Higgins, C. Kiyanda, H. Ng, N. Nikiforakis, Effect of spatial inhomogeneities on detonation propagation with yielding confinement, Shock Waves 28 (5) (2018) 993–1009.
[14] A. Cuadra, C. Huete, M. Vera, Effect of equivalence ratio fluctuations on planar detonation discontinuities, J. Fluid Mech. 903 (2020) A30.
[15] Y. Wang, Z. Chen, H. Chen, Propagation of gaseous detonation in spatially inhomogeneous mixtures, Phys. Fluids 33 (11) (2021) 116105.
[16] P.C. Ma, Y. Lv, M. Ihme, An entropy-stable hybrid scheme for simulations of transcritical real-fluid flows, J. Comput. Phys. 340 (2017) 330–357.
[17] D.G. Goodwin, H.K. Moffat, I. Schoegl, R.L. Speth, B.W. Weber, Cantera: An object-oriented software toolkit for chemical kinetics, thermodynamics, and transport processes, 2022Version 2.6.0.
[18] H. Wu, P.C. Ma, M. Ihme, Efficient time-stepping techniques for simulating turbulent reactive flows with stiff chemistry, Comput. Phys. Commun. 243 (2019) 81–96.
[19] M. Frederick, R. Gejji, J. Shepherd, C.D. Slabaugh, Statistical analysis of methane detonation wave structure in a narrow channel, AIAA Paper, 2021. 2021–0800
[20] L. Wang, H. Ma, Z. Shen, B. Xue, Y. Cheng, Z. Fan, Experimental investigation of methane-oxygen detonation propagation in tubes, Appl. Therm. Eng. 123 (2017) 1300–1307.
[21] C. Wang, C. Qian, J. Liu, M.A. Liberman, Influence of chemical kinetics on detonation initiating by temperature gradients in methane/air, Combust. Flame 197 (2018) 400–415.
[22] P.C. Ma, H. Wu, J.W. Labahn, T. Jaravel, M. Ihme, Analysis of transient blow-out dynamics in a swirl-stabilized combustor using large-eddy simulations, Proc. Combust. Inst. 37 (2019) 5073–5082.

Please cite this article as: D. Brouzet, G. Vignat and M. Ihme, Dynamics and structure of detonations in stratified product-gas diluted mixtures, Proceedings of the Combustion Institute, https://doi.org/10.1016/j.proci.2022.07.173

[23] E. Hu, X. Li, X. Meng, Y. Chen, Y. Cheng, Y. Xie, Z. Huang, Laminar flame speeds and ignition delay times of methane/air mixtures at elevated temperatures and pressures, Fuel 158 (2015) 1–10.
[24] V.N. Gamezo, D. Desbordes, E.S. Oran, Formation and evolution of two-dimensional cellular detonations, Combust. Flame 116 (1–2) (1999) 154–165.
[25] N. Odier, M. Sanjosé, L. Gicquel, T. Poinsot, S. Moreau, F. Duchaine, A characteristic inlet boundary condition for compressible, turbulent, multispecies turbomachinery flows, Comput. Fluids 178 (2019) 41–55.
[26] G.J. Sharpe, Transverse waves in numerical simulations of cellular detonations, J. Fluid Mech. 447 (2001) 31–51.
[27] J.E. Shepherd, Shock and Detonation Toolbox, https://shepherd.caltech.edu/EDL/PublicResources/sdt, 2021.
[28] M.I. Radulescu, G.J. Sharpe, C.K. Law, J.H. Lee, The hydrodynamic structure of unstable cellular detonations, J. Fluid Mech. 580 (2007) 31–81.
[29] M. Radulescu, G. Sharpe, J. Lee, C. Kiyanda, A. Higgins, R. Hanson, The ignition mechanism in irregular structure gaseous detonations, Proc. Combust. Inst. 30 (2005) 1859–1867.
[30] J. Li, X. Mi, A.J. Higgins, Effect of spatial heterogeneity on near-limit propagation of a pressure-dependent detonation, Proc. Combust. Inst. 35 (2015) 2025–2032.

Please cite this article as: D. Brouzet, G. Vignat and M. Ihme, Dynamics and structure of detonations in stratified product-gas diluted mixtures, Proceedings of the Combustion Institute, https://doi.org/10.1016/j.proci.2022.07.173